

# UNCLASSIFIED

AD NUMBER
AD236085
NEW LIMITATION CHANGE
TO Approved for public release, distribution unlimited
FROM Distribution authorized to U.S. Gov't. agencies and their contractors; Administrative/Operational Use; FEB 1960. Other requests shall be referred to Air Force Cambridge Research Laboratories, Hanscom AFB, MA.
AUTHORITY
AFCRL ltr, 3 Nov 1971

THIS PAGE IS UNCLASSIFIED

# UNCLASSIFIED

# AD

# 236 085

Reproduced

## Armed Services Technical Information Agency

ARLINGTON HALL STATION; ARLINGTON 12 VIRGINIA

NOTICE: WHEN GOVERNMENT OR OTHER DRAWINGS, SPECIFICATIONS OR OTHER DATA ARE USED FOR ANY PURPOSE OTHER THAN IN CONNECTION WITH A DEFINITELY RELATED GOVERNMENT PROCUREMENT OPERATION, THE U. S. GOVERNMENT THEREBY INCURS NO RESPONSIBILITY, NOR ANY OBLIGATION WHATSOEVER; AND THE FACT THAT THE GOVERNMENT MAY HAVE FORMULATED, FURNISHED, OR IN ANY WAY SUPPLIED THE SAID DRAWINGS, SPECIFICATIONS, OR OTHER DATA IS NOT TO BE REGARDED BY IMPLICATION OR OTHERWISE AS IN ANY MANNER LICENSING THE HOLDER OR ANY OTHER PERSON OR CORPORATION, OR CONVEYING ANY RIGHTS OR PERMISSION TO MANUFACTURE, USE OR SELL ANY PATENTED INVENTION THAT MAY IN ANY WAY BE RELATED THERETO.

# UNCLASSIFIED

NOTICE: When government or other drawings, specifications or other data are used for any purpose other than in connection with a definitely related government procurement operation, the U. S. Government thereby incurs no responsibility, nor any obligation whatsoever; and the fact that the Government may have formulated, furnished, or in any way supplied the said drawings, specifications, or other data is not to be regarded by implication or otherwise as in any manner licensing the holder or any other person or corporation, or conveying any rights or permission to manufacture, use or sell any patented invention that may in any way be related thereto.

AD No. 236 08

ASTIA FILE COPY

(1)

# A LEAKY-WAVE ANTENNA WITH A CURVED APERTURE

By: R. C. Honey and J. K. Shimizu

Prepared for:

AIR FORCE CAMBRIDGE RESEARCH CENTER AIR RESEARCH AND DEVELOPMENT COMMAND  
LAURENCE G. HANSCOM FIELD BEDFORD, MASSACHUSETTS

STANFORD RESEARCH INSTITUTE

MENLO PARK, CALIFORNIA



FILE COPY

Return to

ASTIA

ARLINGTON HALL STATION

ARLINGTON 12, VIRGINIA

NOX

**Best  
Available  
Copy**



February 1960

Scientific Report 5

# **A LEAKY-WAVE ANTENNA WITH A CURVED APERTURE**

By: R. C. Honey and J. K. Shimizu

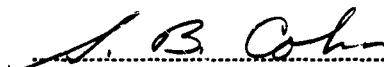
SRI Project 2605

Prepared for:

AIR FORCE CAMBRIDGE RESEARCH CENTER AIR RESEARCH AND DEVELOPMENT COMMAND  
LAURENCE G. HANSCOM FIELD BEDFORD, MASSACHUSETTS

Contract AF 19(604)-3502

Approved:

  
S. B. COHN, MANAGER ELECTROMAGNETICS LABORATORY

  
D. R. SCHEUCH, ASSISTANT DIRECTOR OF ENGINEERING RESEARCH

Copy No. 35

## ABSTRACT

---

The design and the measured performance of a leaky-wave antenna whose radiating aperture is curved to fit flush with a 30-degree sector of a cylindrical surface are presented. The radius of curvature of the surface is about 46 inches, or 44 wavelengths at the design frequency. The aperture of this antenna is 18 inches in the *E*-plane with an arc length of 24 inches in the *H*-plane, and consists of an inductive sheet spaced over a conducting surface.

The radiation patterns of this antenna were measured over the frequency range 8 to 13 kMc. At the design frequency, 11.42 kMc, the experimental results check extremely well with the theoretical predictions for a pencil beam 3.8-degrees wide in the *H*-plane by 3-degrees in the *E*-plane, tilted 55-degrees in the *H*-plane from the normal to the surface at the feed end of the antenna.

## CONTENTS

---

ABSTRACT . . . . .	ii
LIST OF ILLUSTRATIONS . . . . .	iv
 I INTRODUCTION . . . . .	 1
II MEASURED PERFORMANCE . . . . .	2
A. General . . . . .	2
B. Radiation Patterns . . . . .	5
C. Gain . . . . .	13
D. Input Impedance . . . . .	14
III ELECTRICAL DESIGN . . . . .	15
A. General . . . . .	15
B. Design Procedure . . . . .	16
C. Line Source Feed . . . . .	18
IV CONCLUSIONS . . . . .	23
REFERENCES . . . . .	24



## ILLUSTRATIONS

---

Fig. 1	Cylindrical Contoured Leaky-Wave Antenna . . . . .	2
Fig. 2	Sketch of Antenna Geometry . . . . .	3
Fig. 3	Photograph Showing the Antenna with the Line Source Feed . . . . .	4
Fig. 4	H-Plane Coordinate System . . . . .	5
Fig. 5	Comparison of Experimental and Theoretical H-Plane Radiation Patterns at 11.42 kMc. . . . .	7
Fig. 6	H-Plane Radiation Patterns . . . . .	8
Fig. 7	Scan Angle vs. Frequency . . . . .	10
Fig. 8	H-Plane Beamwidth vs. Frequency . . . . .	11
Fig. 9	E-Plane Radiation Patterns . . . . .	12
Fig. 10	E-Plane Beamwidth vs. Frequency . . . . .	13
Fig. 11	Gain vs. Frequency . . . . .	14
Fig. 12	Input VSWR vs. Frequency . . . . .	14
Fig. 13	The Guide Wavelength, $\lambda/\lambda_g$ , Along the Antenna Aperture . . . . .	17
Fig. 14	Amplitude Distribution Along the Antenna Aperture . . . . .	19
Fig. 15	Radiation Along the Antenna Aperture . . . . .	19
Fig. 16	The Wire Spacing $s$ as a Function of $\theta$ for $D = 0.005$ In. . . . .	20
Fig. 17	The Cavity Height $s$ as a Function of $\theta$ . . . . .	21
Fig. 18	Horizontally Polarized Line Source . . . . .	22

## TABLE

Table 1	Characteristics of the Theoretical and Experimental Radiation Patterns at the Frequency of 11.42 kMc . . . . .	6
---------	---	---

# A LEAKY-WAVE ANTENNA WITH A CURVED APERTURE

## I INTRODUCTION

Certain types of leaky-wave antennas have been shown to produce accurately controlled and highly predictable radiation patterns when mounted so that the aperture lies on a flat surface.<sup>1,2,3</sup> This report will show that very precise control of the radiation pattern can also be obtained in practice when the antenna is curved in the *H*-plane to fit on a singly-curved surface. This is demonstrated by constructing an antenna similar to those described previously,<sup>1,2,3</sup> but curved in the *H*-plane to form a 30-degree sector of a cylindrical surface. As before, the antenna consists of an array of parallel conducting wires spaced over a suitably curved conducting surface. The antenna is 18 inches wide in the *E*-plane and has an arc-length of 24 inches in the *H*-plane, with a radius of curvature equal to 45.8 inches. It is fed from one end with the same line-source described previously,<sup>2,3</sup> and radiates a pencil beam designed to be 3.8 degrees wide in the *H*-plane and 3 degrees wide in the *E*-plane at the design frequency, 11.42 kMc.

Section II of this report presents the measured data taken on the antenna over the band from 8 to 13 kMc, and Sec. III explains the design procedure used to compensate for the curvature of the surface while radiating a pencil beam.

## II MEASURED PERFORMANCE

### A. GENERAL

The leaky-wave antenna that was built to check the theoretical predictions and the design procedure is shown in the photograph of Fig. 1. The aperture of this antenna is 18 inches wide in the *E*-plane and is curved to fit a cylindrical surface with an arc length of 24 inches in the *H*-plane. This arc length is equal to a 30-degree sector of a cylindrical surface having a radius of 45.8 inches. As shown in Fig. 1, a large number of parallel wires 0.005 inches in diameter are stretched across the aperture with the spacing between adjacent wires varied along the 24-inch arc length. Figure 1 also shows that the spacing of this wire grid over the conducting surface varies along the length of the aperture; the spacing is varied in order to maintain a constant phase across the aperture projected onto a plane surface. This spacing between the wire grid and the conducting surface decreases from 0.900 inches at



FIG. 1

CYLINDRICAL CONTOURED LEAKY-WAVE ANTENNA

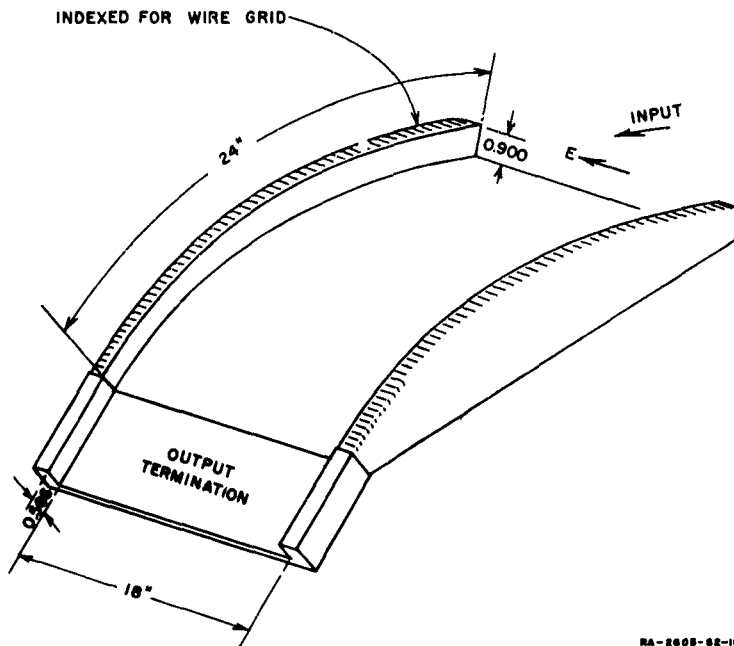


FIG. 2  
SKETCH OF ANTENNA GEOMETRY

the input terminal to 0.566 inches at the output terminal, as shown in the sketch of Fig. 2. Qualitatively, the spacing between adjacent wires controls the amplitude of the illumination along the aperture, while the spacing between the wire grid and the conducting surface controls the phase velocity along the antenna. The spacing between the wire grid and the conducting surface controls the phase velocity in much the same way that the width of conventional rectangular waveguide controls the phase velocity in the waveguide.

This antenna, complete with line-source feed, is shown mounted on the antenna pattern range in Fig. 3. The line-source feed used here is a hoghorn having an aperture of 0.900 inches by 18.00 inches wide, the design of which is described in Refs. 2 and 3.

A series of measurements of this antenna was taken over a frequency range of 8 to 13 kMc. These measurements are described in this section and are compared with the theoretical predictions at the design frequency.

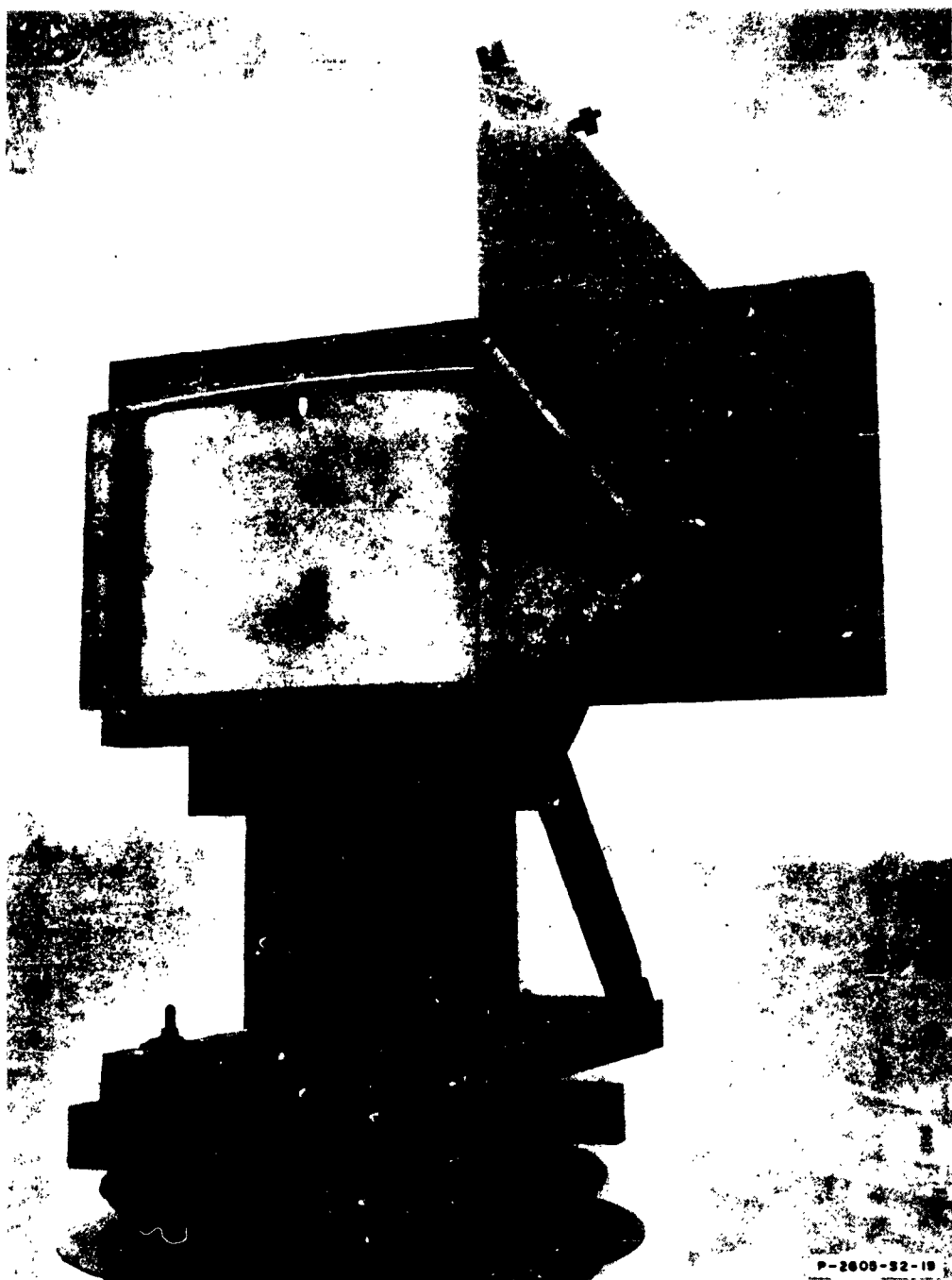


FIG. 3  
PHOTOGRAPH SHOWING THE ANTENNA WITH THE LINE SOURCE FEED

## B. RADIATION PATTERNS

The theoretical radiation pattern of this antenna at the design frequency was found approximately by projecting the curved aperture onto a flat plane, then calculating the radiation pattern from this flat aperture in the usual way. The phase velocity along the curved surface was varied along the aperture so that the radiation from every point in the aperture was directed in the same direction in space, in this case,  $54^\circ 58'$  from the normal to the surface at the feed end of the aperture as shown in Fig. 4. There are two plane projected apertures shown in Fig. 4, one of length  $L$  which is a chord of the cylindrical surface, and one of length  $L_p$  which is normal to the direction of propagation. The amplitude of the radiation along the curved surface was adjusted to give a sinusoidal amplitude distribution along either projected aperture. The theoretical radiation pattern was then computed as though the radiation occurred from the plane aperture  $L$  at an angle  $\phi - (\theta_0/2)$  or

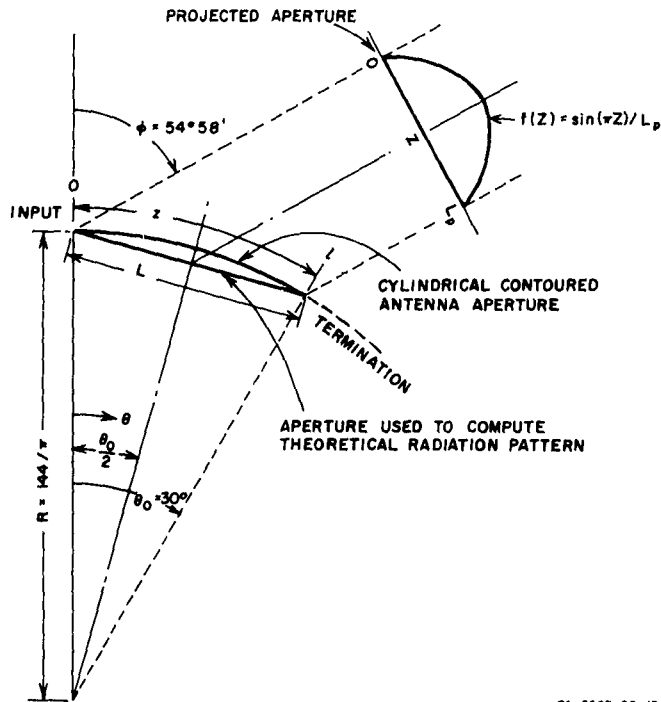


FIG. 4  
H-PLANE COORDINATE SYSTEM

39° 58' from its normal. The amplitude of the pattern from such an aperture, neglecting the element factor, is given by Silver<sup>4</sup> as

$$g(u) = \frac{\cos u}{1 - \frac{4u^2}{\pi^2}} \quad (1)$$

where  $u$  is the normalized angular variable and is equal to

$$u = \frac{\pi L}{\lambda} [\sin(\theta - 15^\circ) - \sin(39^\circ 58')] \quad (2)$$

The final pattern is then found from

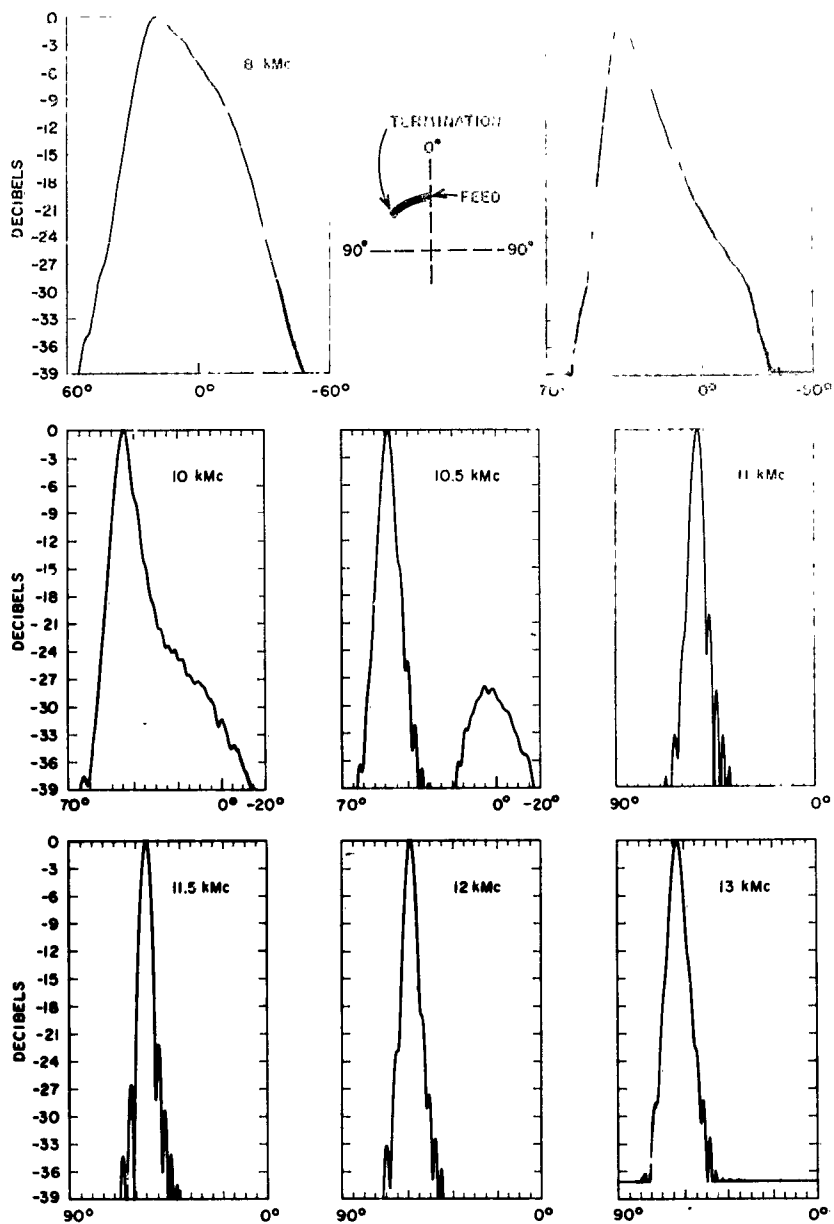
$$p(\theta) = \frac{\cos^2 u \cos^2(\theta - 15^\circ)}{\left(1 - \frac{4u^2}{\pi^2}\right)} \quad (3)$$

where  $\cos(\theta - 15^\circ)$  is the H-plane element factor for a magnetic dipole oriented in the direction of propagation along the infinite, flat conducting plane. This pattern, normalized to unity at the peak of the beam is shown on the left in Fig. 5 with the angle  $\theta$  on the abscissa. This pattern is to be compared with the experimental H-plane pattern measured at the design frequency, 11.42 kMc, which is shown on the right in Fig. 5. It can be seen that the agreement between the two patterns is extremely good. Table I summarizes the important characteristics of these two patterns.

H-plane radiation patterns were measured at a number of other frequencies from 8 to 13 kMc. A typical series of patterns is shown in Fig. 6. As seen from these radiation patterns, the beam from the antenna scans in the H-plane with frequency. This scanning action is due to the

TABLE I  
CHARACTERISTICS OF THE THEORETICAL AND  
EXPERIMENTAL RADIATION PATTERNS AT THE  
FREQUENCY OF 11.42 kMc

	THEORETICAL	EXPERIMENTAL
Tilt angle, $\phi$	54° 58'	55°
Half-power Bandwidth	3.8°	3.7°
1st Side Lobes	-22.3 db -24.0 db	-22.2 db -26.0 db



RB-2605-92-4

FIG. 6  
H-PLANE RADIATION PATTERNS



the beamwidth of the antenna as a function of frequency is shown in Fig. 7. The radiation patterns of Fig. 6 also show that the experimental half-power beamwidth remains fairly constant between 10.5 to 13 kMc, but increases as the frequency is decreased from 10.5 to 8 kMc. A curve showing the frequency dependence of the beamwidth is shown in Fig. 8. The effect on the beamwidth as a function of frequency can be explained in terms of the projected aperture,  $L_p$ . In the frequency range where the beamwidth remains fairly constant, the projected aperture also remains approximately constant in wavelengths. However, below 10.5 kMc the progressive increase in the beamwidth is due to the diminishing projected aperture as the frequency is lowered. This decrease in the projected aperture results from the fact that more and more of the antenna towards the load end becomes cut-off as the frequency decreases. In Sec. III, this cut-off is determined by the spacing,  $a$ , between the wire grid and the conducting surface, and for this antenna,  $a$  decreases from 0.900 inches at the input terminal to 0.566 inches at the termination.

The antenna was designed so that 15 percent of the power is absorbed by the load termination at the design frequency. However, due to the cut-off condition encountered near the termination at frequencies below 10.5 kMc, this power is not absorbed by the load, but reflected back down the antenna and radiated. This radiation appears as a secondary lobe near the normal ( $0^\circ$ ) to the antenna as shown in Fig. 6. The radiation patterns of Fig. 6 show that below 10 kMc this reflection lobe merges with the main lobe of the antenna pattern producing smoothly varying patterns which show promise for some shaped-beam applications.

The E-plane radiation patterns of the antenna are essentially identical to the E-plane patterns of the line source used to feed the antenna and are shown in Fig. 9. The measured values of the E-plane beamwidths for the complete antenna are compared in Fig. 10 with the beamwidths of the line-source alone and to the theoretical beamwidth for a perfect line-source of this type. The measured first side-lobe levels vary from 13.8 to 16.8 db below the main beam as compared to the 13.8 db first side lobe level of a uniformly illuminated aperture.

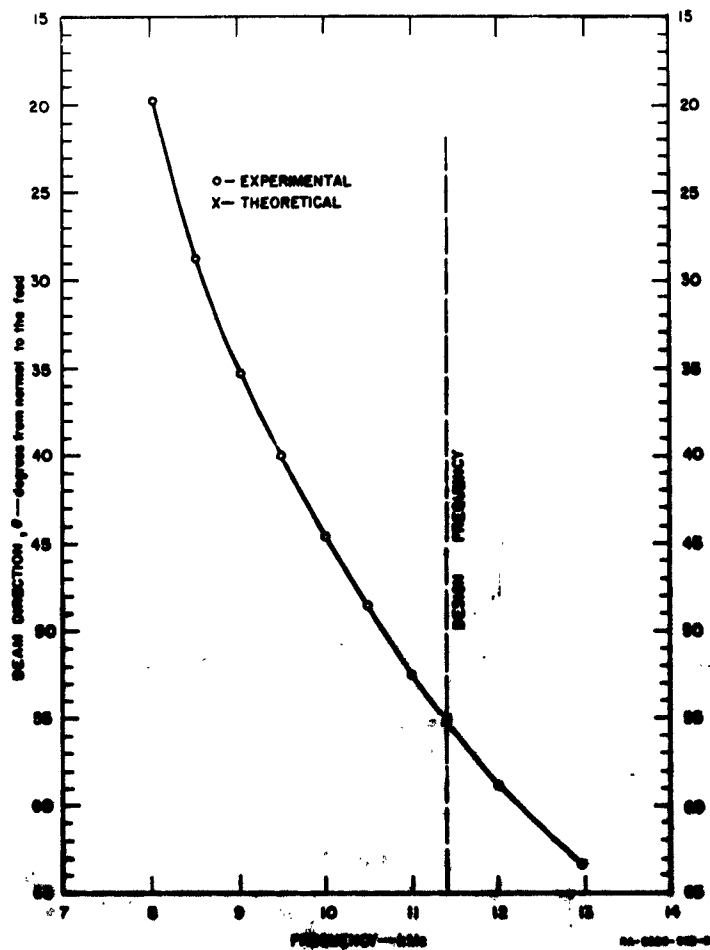


FIG. 7  
 SCAN ANGLE VS FREQUENCY

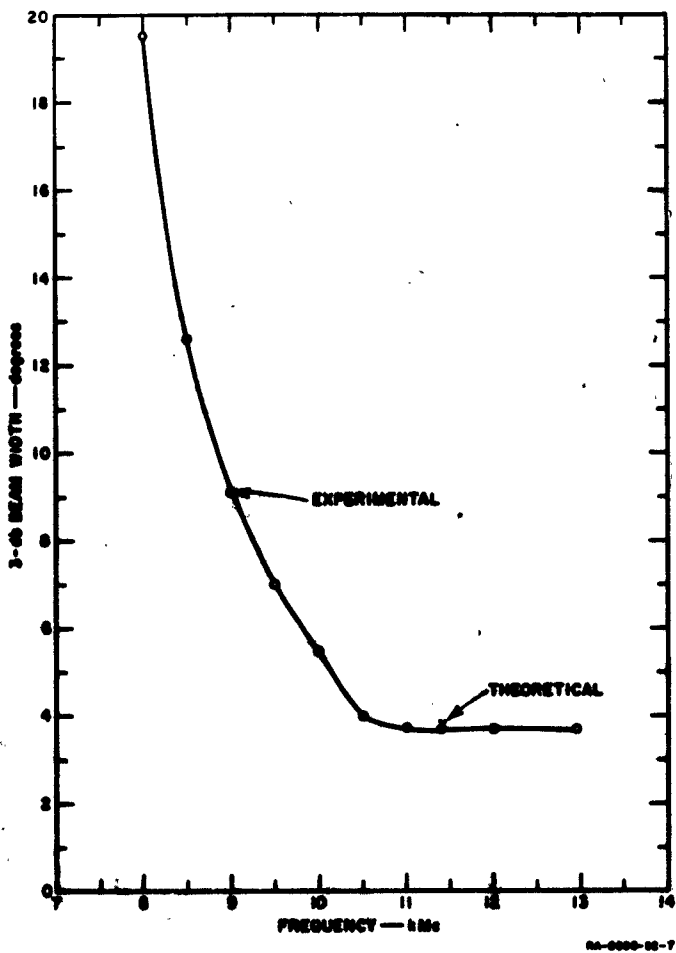


FIG. 8  
H-PLANE BEAMWIDTH VS FREQUENCY

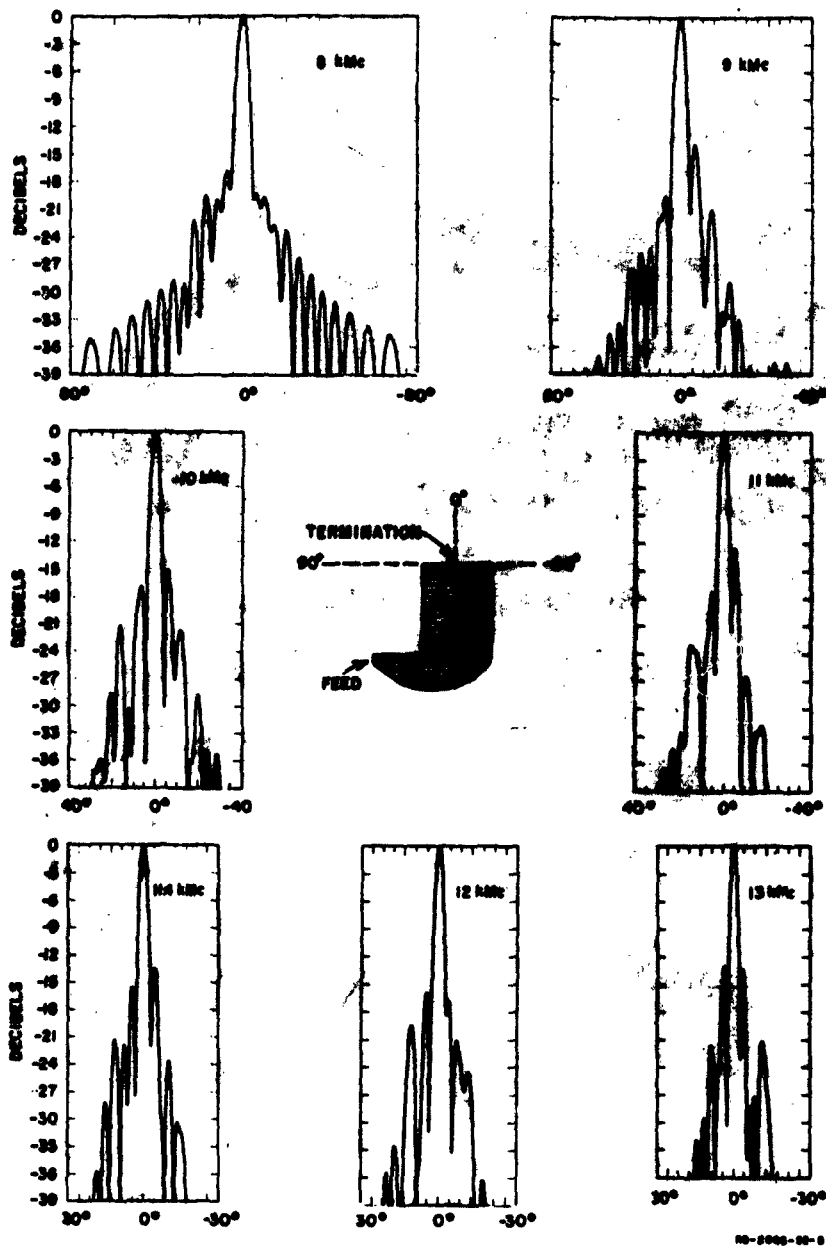


FIG. 9  
E-PLANE RADIATION PATTERNS

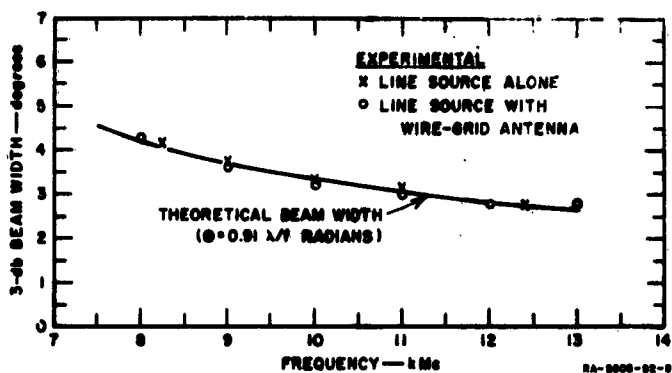


FIG. 10  
E-PLANE BEAMWIDTH VS FREQUENCY

### C. GAIN

The gain of the wire-grid antenna was carefully measured by comparing the gain with that of a standard horn. The results of these measurements are shown plotted in Fig. 11, along with the theoretical directivity computed at the design frequency of 11.42 kMc. The theoretical gain was calculated assuming linear phase distribution in both planes—that is,

$$G = 4\pi \left( \frac{l}{\lambda} \right)_{eff} \left( \frac{f}{\lambda} \right)_{eff} G_E G_H = 4\pi \left( \frac{L_P}{\lambda} \right) \left( \frac{f}{\lambda} \right) G_E G_H F \quad (4)$$

$$= 24.22 \text{ db}$$

where

$L_P$  is the projected aperture in the H-plane and is equal to 18.1847 inches

$f$  is the length of the aperture in the E-plane and is equal to 18.00 inches

$G_E$  is the gain factor in the E-plane and is equal to 0.9954 (Refs. 2 and 3)

$G_H$  is the gain factor in the H-plane which is given by Silver<sup>4</sup> for sinusoidal aperture distributions,  $G_H = 0.810$

$F$  is the fraction of the input power radiated by the antenna— $F = 0.85$  in this case.

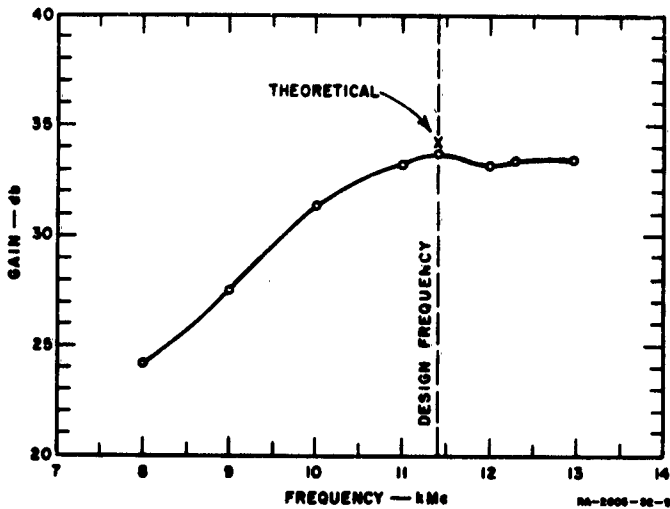


FIG. 11  
GAIN VS FREQUENCY

#### D. INPUT IMPEDANCE

The results of the input VSWR measurements of the wire-grid antenna plus the line-source feed over the frequency band of 8 to 13 kMc are shown in Fig. 12. The high VSWR measured at the low end of the frequency band is due to the termination of the antenna being below cut-off. At other frequencies in the band, the input impedance of the complete antenna is determined by the impedance of the line-source feeding the antenna. The input VSWR of the line source alone was less than 1.1 over the frequency band of 7 to 13 kMc.

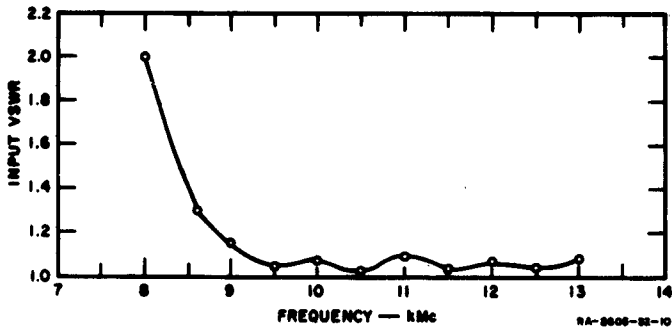


FIG. 12  
INPUT VSWR VS FREQUENCY

### III ELECTRICAL DESIGN

#### A. GENERAL

In this section the procedure for designing the leaky-wave antenna described in this report is presented. First of all, the radiating surface of this antenna was arbitrarily chosen to have a cylindrical contour of radius  $R$  with the length of the antenna aperture being a  $\theta_0$ -degree sector of this cylindrical surface. At the design frequency, the main beam of the radiation pattern was then selected to point at an angle  $\phi$  from the normal to the feed as shown in Fig. 4. In order to have the radiation from each portion of the antenna add up in phase in the direction of the main beam,  $\phi$ , it is necessary that the guide wavelength,  $\lambda_g$ , vary along the antenna as

$$\lambda/\lambda_g = \sin(\phi - \theta) \quad (5)$$

where  $\lambda$  is the free-space wavelength,  $\theta$  is the variable angle, and  $\phi$  is the fixed angle associated with the direction of the main beam.

The aperture distribution at the antenna surface that was chosen for this antenna is in the form of

$$g(\theta) = \sin\left\{\frac{\pi R}{L_p} [\sin(\theta - \phi) + \sin\phi]\right\} = \sin\left\{\frac{2\pi R}{L_p} \left[\sin\frac{\theta}{2} \cos\left(\phi - \frac{\theta}{2}\right)\right]\right\} \quad (6)$$

Equation (6) is given in terms of  $L_p$ , where  $L_p$  is the total length of the projected aperture of the radiating surface, and is equal to:

$$L_p = R[\sin(\theta_0 - \phi) + \sin\phi] = 2R \sin\frac{\theta_0}{2} \cos\left(\phi - \frac{\theta_0}{2}\right) \quad (7)$$

This projected aperture lies on a constant phase plane, and is perpendicular to the direction of the main beam as shown in Fig. 4. The aperture distribution given by Eq. (6) is the result of the prescribed sinusoidal amplitude distribution

$$f(Z) = \sin \frac{\pi Z}{L_p} \quad (8)$$

on the constant phase plane projected on to the cylindrical contour of the radiating surface.

For an end-fed linear array, the aperture distribution is related to the effective attenuation or radiation constant,  $\alpha(z)$ , along the array in the following way:<sup>2,3</sup>

$$\begin{aligned} 2\alpha(z) &= \frac{g^2(z)}{\frac{1}{F} \int_0^l g^2(\xi) d\xi - \int_0^z g^2(\xi) d\xi} \\ &= \frac{g^2(\theta)}{\frac{R}{F} \int_0^{\theta_0} g^2(\theta) d\theta - R \int_0^\theta g^2(\theta) d\theta} \text{ nepers/unit distant} \end{aligned} \quad (9)$$

where  $\xi$  is the variable of integration along the aperture and  $F$  is the fraction of the input power that is radiated by the antenna. This formulation neglects the losses in the array due to the finite conductivity of the metal, which, of course, is a safe assumption in this case.

## B. DESIGN PROCEDURE

This section of the report describes the steps taken to design the leaky-wave antenna discussed above.

First, the size of the antenna aperture was chosen to be 18 inches wide in the E-plane with an arc length,  $l$ , of 24 inches in the H-plane. This arc length was then chosen to be a 30-degree sector of a cylindrical surface, making the radius,  $R$ , of this cylindrical contour equal to  $144/\pi$  or 45.8 inches long.

A design frequency of 11.42 kMc was then arbitrarily selected and an initial  $a$  dimension of 0.900 inches chosen for the unperturbed guide that matched the line source. At this frequency,



$$\begin{array}{lcl}
 \lambda & = & 2.624 \text{ cm} = 1.033 \text{ in.} \\
 \lambda_g & = & 3.205 \text{ cm} = 1.262 \text{ in.} \\
 \lambda/\lambda_g & = & 0.8188 \\
 \lambda/2a & = & 0.5741
 \end{array}
 \left. \vphantom{\begin{array}{l} \lambda \\ \lambda_g \\ \lambda/\lambda_g \\ \lambda/2a \end{array}} \right\} \text{ unperturbed guide}$$

The direction of the main beam,  $\phi$ , of the radiation pattern is found from  $\sin \phi = \lambda/\lambda_g$ , or  $\phi = 54^\circ 58'$ , and the variation of  $\lambda/\lambda_g$  along the aperture is found from Eq. (5) and is shown plotted in Fig. 13.

Knowing the radius,  $R$ , and the angles  $\theta_0$  and  $\phi$ , the aperture distribution  $g(\theta)$  given in Eq. (6) reduces to

$$g(\theta) = \sin 7.881 [\sin (\theta - 54^\circ 58') + 0.8148] \quad (10)$$

and the total length of the projected aperture,  $L_p = 18.18$  inches at 11.42 kMc. A plot of  $g(\theta)$  is shown in Fig. 14.

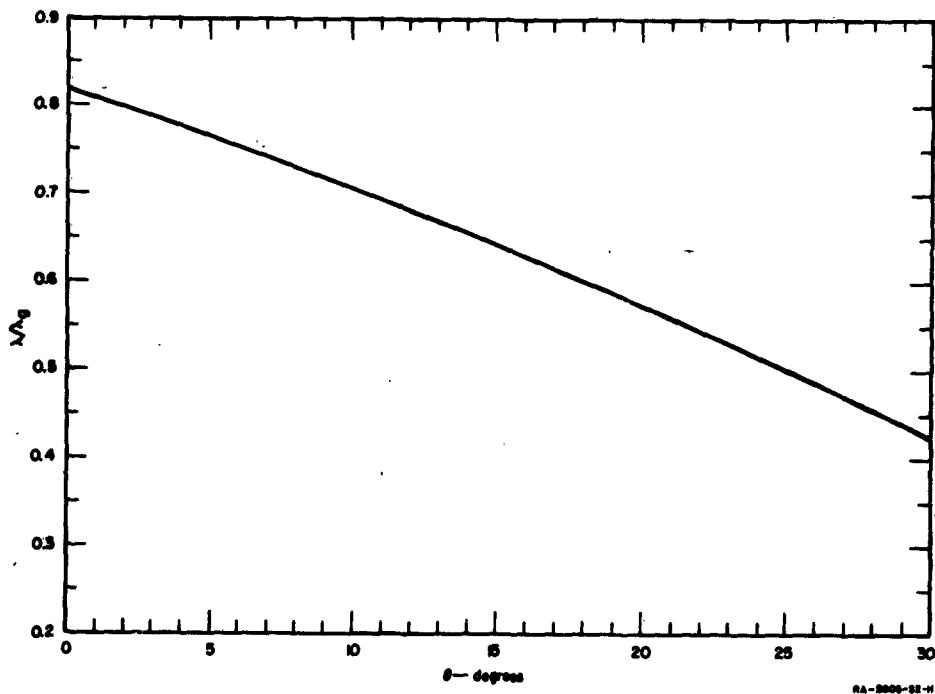


FIG. 13  
THE GUIDE WAVELENGTH,  $\lambda/\lambda_g$ , ALONG THE ANTENNA APERTURE

Knowing the function  $g(\theta)$ , the value of  $2la(z)$  was then determined from Eq. (9) with  $F = 0.85$ , and is plotted in Fig. 15.

The geometry of the wire grid—i.e., wire size and spacing, required to produce the values of  $\alpha$ , and the spacing of the grid over the conducting surface which is required to produce the values of  $\lambda/\lambda_g$ , (see Figs. 13 and 15)—can then be found from the design data published previously.<sup>2,3</sup> For instance, given  $\lambda = 1.033$  inches, the factor  $C\lambda/2a$  can be found as a function of aperture position from Fig. 17 in Ref. 3, where  $C/a$  is a real function of the wire grid only, given by

$$\frac{C}{a} = \frac{2\pi}{s \left( \ln \csc \frac{\pi D}{S} + F \right)} \quad (11)$$

where  $D$  is the wire diameter,  $s$  is the wire-to-wire spacing, and  $F$  is a correction factor applied for large wire spacings.<sup>2,3</sup> The wire diameter was arbitrarily selected as  $D = 0.005$  inches, hence the spacing as a function of position along the array is given by Eq. (11), and is shown in Fig. 16. The spacing of the wire grid over the conducting surface can then be found from Fig. 18 in Ref. 3, and this is plotted in Fig. 17.

#### C. LINE SOURCE FEED

The line source used to feed this antenna was the same line source used for the earlier flat leaky-wave antenna and described in detail previously.<sup>2,3</sup> It consists simply of an asymmetrically fed pillbox between parallel planes spaced 0.900 inch apart, and is shown in Fig. 18.

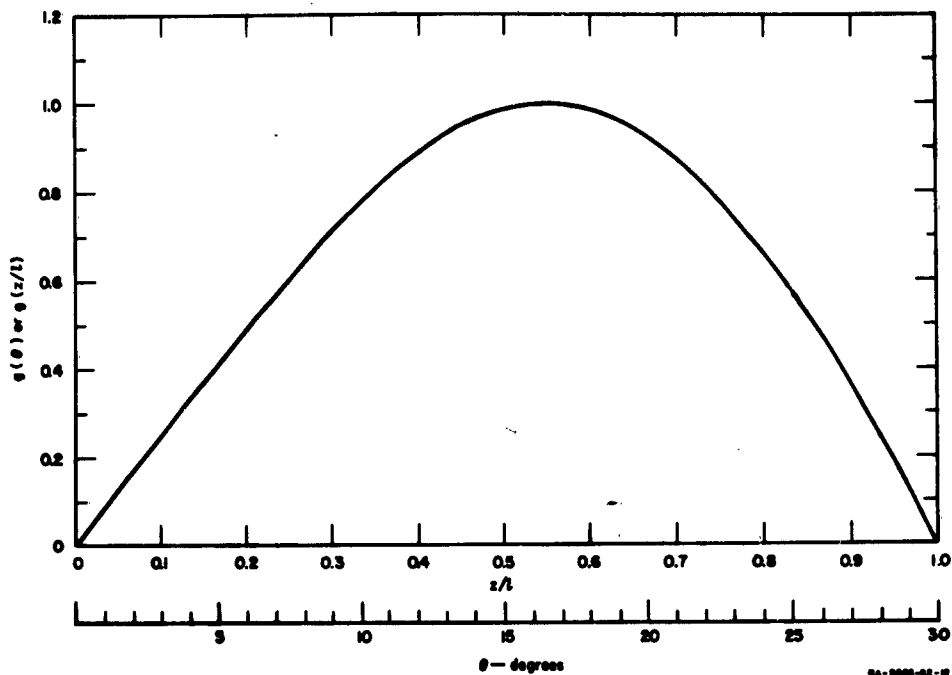


FIG. 14  
AMPLITUDE DISTRIBUTION ALONG THE ANTENNA APERTURE

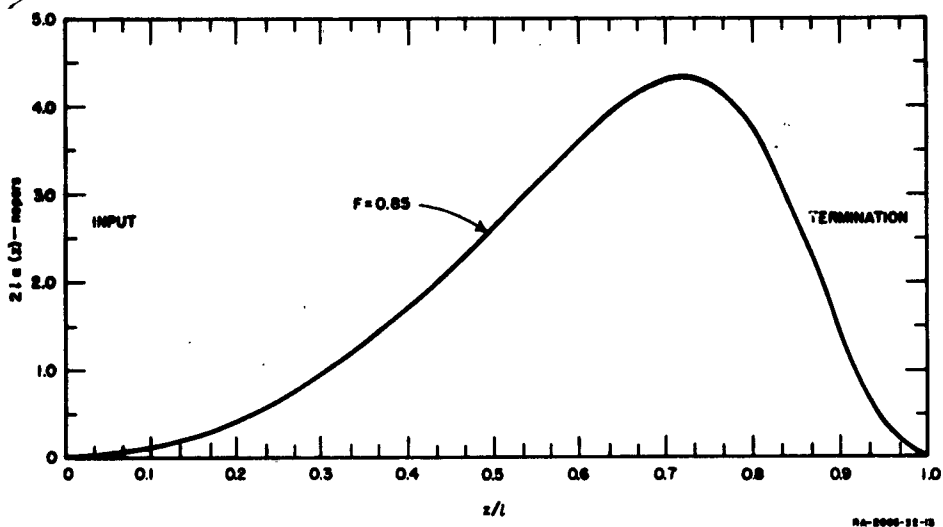


FIG. 15  
RADIATION ALONG THE ANTENNA APERTURE

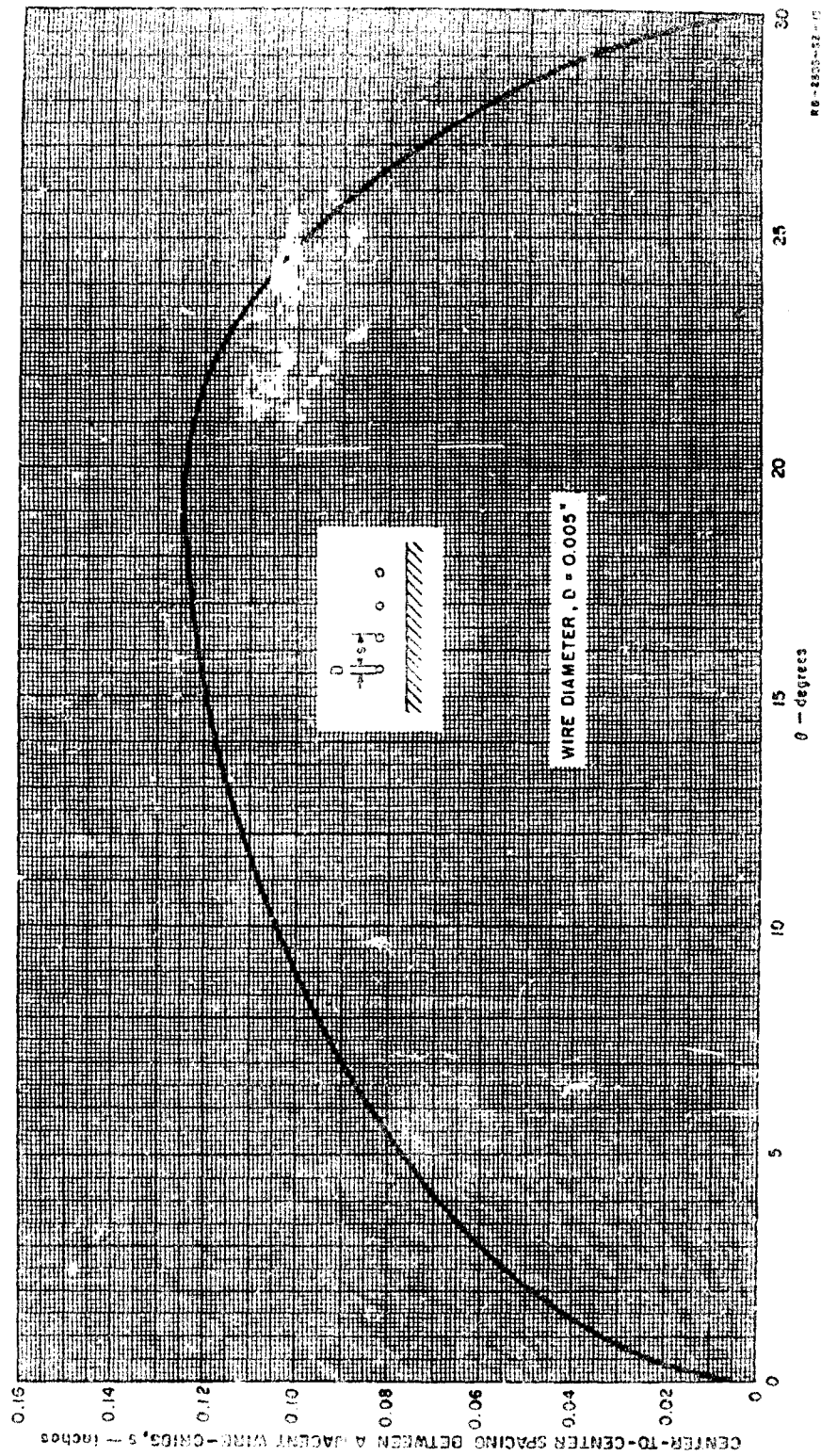


FIG. 16  
THE WIRE SPACING  $s$  AS A FUNCTION OF  $\theta$  FOR  $D = 0.005$  IN.

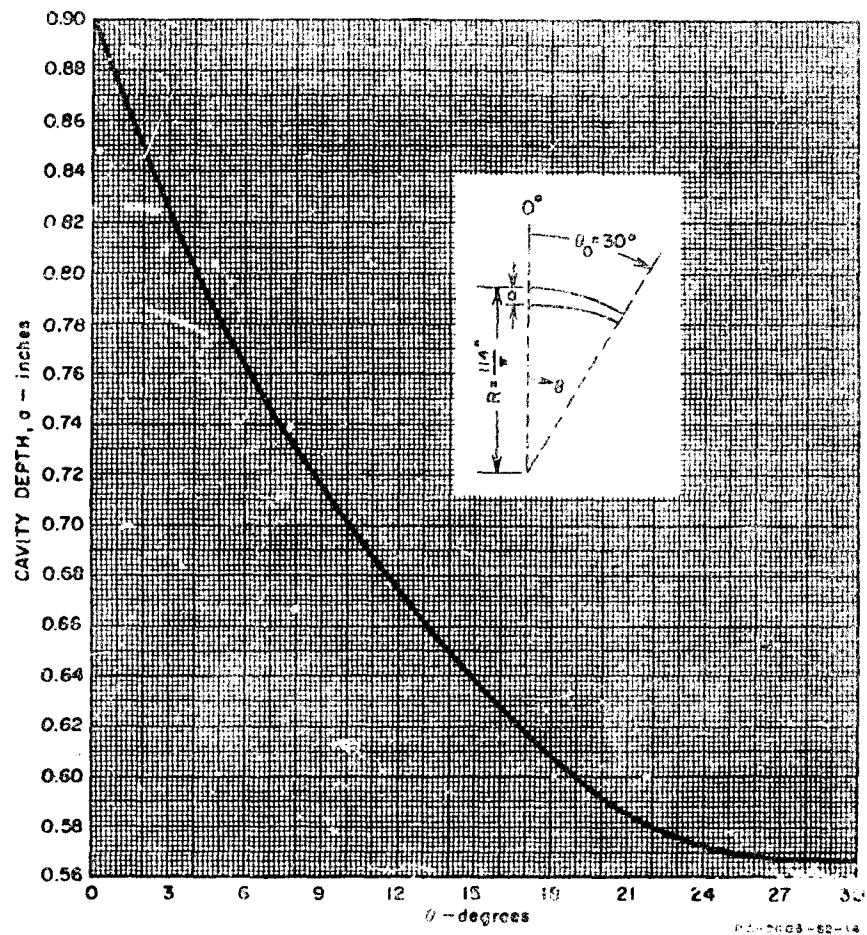
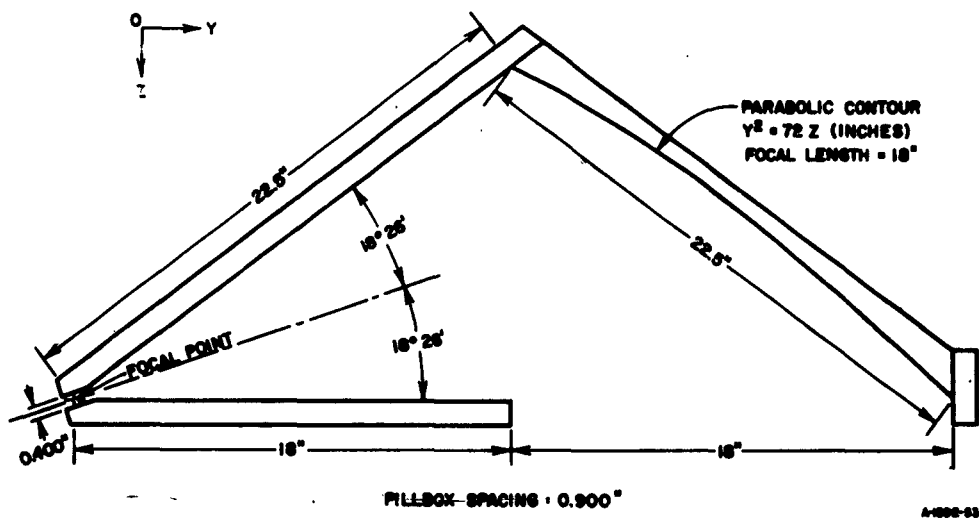


FIG. 17  
THE CAVITY HEIGHT  $a$  AS A FUNCTION OF  $\theta$



**FIG. 18**  
**HORIZONTALLY POLARIZED LINE SOURCE**

#### IV CONCLUSIONS

It had been shown previously<sup>2,3</sup> that the behavior of this leaky-wave structure on a flat surface could be very precisely predicted, thus permitting independent and precise control of the phase and amplitude distributions across a flat antenna aperture. The present antenna has shown that control nearly as precise can be obtained when the antenna is curved gradually in the H-plane to fit flush with a curved surface. It is apparent that an appreciably smaller radius of curvature could be utilized before the errors would become significant in most applications. It follows, then, that leaky-wave antennas of this type can be designed to fit any singly curved surface whose radii of curvature along the aperture lie between some lower limit (less than 44 wavelengths) and infinity. They can be designed to radiate pencil-beam or shaped-beam patterns.

It cannot definitely be determined whether the very slight discrepancies that do occur (3 db differences at 40 db down from the main lobe on one side of the beam) are due to approximations made in predicting the radiation from a curved surface, to approximations made in the design of the leaky-wave structure, to finite tolerances in the construction of the experimental antenna, or to combinations of these factors.

Although the antenna described here was constructed by stretching large numbers of parallel wires across the aperture, the wire grid can be replaced by a grid of flat strips photo-etched on a Teflon-Fiberglass laminate,<sup>2,3</sup> by letting the width of the flat strips equal twice the diameter of the round wires.

## REFERENCES

1. R. C. Honey, "A Flush-Mounted Horizontally-Polarized Directional Antenna," Tech. Report 54, SRI Project 1197, Contract AF 19(604)-1296, Stanford Research Institute, Menlo Park, California (January 1956).
2. R. C. Honey, "A Flush-Mounted Leaky-Wave Antenna with Predictable Patterns," Scientific Report 4, SRI Project 1592, Contract AF 19(604)-1571, Stanford Research Institute, Menlo Park, California (June 1958).
3. R. C. Honey, "A Flush-Mounted Leaky-Wave Antenna with Predictable Patterns," *IRE Trans., PGAP-7*, 4, pp. 320-329 (October 1959).
4. S. Silver, *Microstrip Antenna Theory and Design*, Chap. 6, MIT Rad. Lab. Series, Vol. 12 (McGraw-Hill Book Co., New York, N.Y., 1949).



**STANFORD  
RESEARCH  
INSTITUTE**

**MENLO PARK, CALIFORNIA**

**REGIONAL OFFICES AND LABORATORIES**

**SOUTHERN CALIFORNIA LABORATORIES**

**820 Mission Street  
South Pasadena, California**

**SOUTHWEST OFFICE**

**3424 North Central Avenue  
Phoenix, Arizona**

**PACIFIC NORTHWEST OFFICE**

**421 S. W. 6th Avenue  
Portland, Oregon**

**WASHINGTON OFFICE**

**711 14th Street N. W.  
Washington, D. C.**

**EUROPEAN OFFICE**

**P. Likanstrasse 37  
Zurich, Switzerland**

**HAWAII OFFICE**

**195 South King Street  
Honolulu, T. H.**

**NEW YORK OFFICE**

**60 East 42nd Street  
New York 17, New York**